

IOWA STATE UNIVERSITY

Digital Repository

Materials Science and Engineering Publications

Materials Science and Engineering

8-24-2006

Anomalous Ionic Conductivity Increase in $\text{Li}_2\text{S} + \text{GeS}_2 + \text{GeO}_2$ Glasses

Youngsik Kim
Iowa State University

Jason Salenga
Iowa State University

Steve W. Martin
Iowa State University, swmartin@iastate.edu

Follow this and additional works at: http://lib.dr.iastate.edu/mse_pubs



Part of the [Ceramic Materials Commons](#), and the [Physical Chemistry Commons](#)

The complete bibliographic information for this item can be found at http://lib.dr.iastate.edu/mse_pubs/52. For information on how to cite this item, please visit <http://lib.dr.iastate.edu/howtocite.html>.

This Article is brought to you for free and open access by the Materials Science and Engineering at Digital Repository @ Iowa State University. It has been accepted for inclusion in Materials Science and Engineering Publications by an authorized administrator of Digital Repository @ Iowa State University. For more information, please contact digirep@iastate.edu.

Anomalous Ionic Conductivity Increase in $\text{Li}_2\text{S} + \text{GeS}_2 + \text{GeO}_2$ Glasses

Youngsik Kim, Jason Saienga, and Steve W. Martin*

Department of Materials Science and Engineering, Iowa State University, 2220 Hoover Hall, Ames, Iowa 50011

Received: January 31, 2006; In Final Form: May 11, 2006

Numerous studies of the ionic conductivities in oxide-doped chalcogenide glasses have shown the anomalous result that the ionic conductivity actually increases significantly (by more than a factor of 10 in some cases) by the initial addition of an oxide phase to a pure sulfide glass. After this initial sharp increase, the conductivity then monotonically decreases with further oxide addition. While this behavior is important to the application of these glasses for Li batteries, no definitive understanding of this behavior has been elucidated. To examine this effect further and more completely, the ionic conductivities of $0.5\text{Li}_2\text{S} + 0.5[(1-x)\text{GeS}_2 + x\text{GeO}_2]$ glasses have been measured on disc-type bulk glasses. The ionic conductivity of the $0.5\text{Li}_2\text{S} + 0.5\text{GeS}_2$ ($x = 0$) glass was observed to increase from $4.3 \times 10^{-5} (\Omega \text{ cm})^{-1}$ to $1.5 \times 10^{-4} (\Omega \text{ cm})^{-1}$ while the activation energy decreased to 0.358 eV from 0.385 eV by the addition of 5 mol % of GeO_2 . Further addition of GeO_2 monotonically decreased the conductivity and increased the activation energy. On the basis of our previous studies of the structure of this glass system, the Anderson and Stuart model was applied to explain the decrease in the activation energy and increase in the conductivity. It is suggested that the “doorway” radius between adjacent cation sites increases slightly (from $\sim 0.29(\pm 0.05) \text{ \AA}$ to $\sim 0.40(\pm 0.05) \text{ \AA}$) with the addition of oxygen to the glass and is proposed to be the major cause in decreasing the activation energy and thereby increasing the conductivity. Further addition of oxides appears to contract the glass structure (and the doorway radius) leading to an increase in the conductivity activation energy and a decrease in the conductivity.

1. Introduction

LiI-doped sulfide glasses, such as the $\text{LiI} + \text{Li}_2\text{S} + \text{P}_2\text{S}_5$,¹ $\text{LiI} + \text{Li}_2\text{S} + \text{B}_2\text{S}_3$,² and $\text{LiI} + \text{Li}_2\text{S} + \text{SiS}_2$ ³ systems, so-called fast ionic conducting (FIC) glasses, are among the best solid electrolytes known and have a high conductivity of $\sim 10^{-3} (\Omega \text{ cm})^{-1}$ at room temperature. Since these conductivities were considered to be suitable for energy storage applications, lithium batteries with these glassy electrolytes have been fabricated.⁴ However, it has been found that LiI-doped glasses are unstable in contact with Li metal used as an anode and a decrease in the cell performance occurs for lithium batteries fabricated with these electrolytes.^{5–8} The addition of iodides to the glass compositions also tends to decrease the chemical durability and thermal stability of the glasses.⁹

Therefore, several directions have been explored to search for glasses with high stability in contact with Li metal combined with a high ionic conductivity. As a result, oxy-sulfide glasses have been explored to solve this problem. In the study of these oxy-sulfide systems, it has been found, for example, that small amounts of lithium oxysalts, Li_xMO_y (where $\text{Li}_x\text{MO}_y = \text{Li}_3\text{PO}_4$, Li_4SiO_4 , Li_3BO_3 , and Li_4GeO_4), doped into the $\text{Li}_2\text{S} + \text{SiS}_2$ glass system are effective in increasing the stability toward Li metal without losing its high conductivity. As a result, these glasses have been considered as one of the most suitable candidate solid electrolytes for rechargeable Li batteries.^{8,10,11} However, these glasses are extremely unstable in ambient air due to the high chemical reactivity of SiS_2 , which decomposes to SiO_2 and generates poisonous H_2S gas when exposed to air or water.¹² It is important therefore to further optimize the

composition of these glasses to maintain their high ionic conductivity and stability in contact with Li metal, but to also improve their atmospheric stability.

In addition to solving the technical problem of improving their atmospheric stability, there also has developed a significant scientific problem with these oxide-doped chalcogenide glasses. As described above, small additions of a lithium oxysalt lead to a significant increase in the Li ion conductivity. In some cases, as little as 5% addition can lead to a 10-fold increase in the ionic conductivity. While this conductivity and physical property improvement is important to the battery application of these glasses, there has yet to be a definitive study of this anomalous conductivity increase in these glasses. It is not clear, for example, whether the added oxysalts work to increase the total number of cations in the glass or whether they work to increase their mobility, or perhaps both.

It is to these two problems, therefore, that the current project addresses. This work is proposed to develop glasses that have better atmospheric stability while at the same time developing a better and more complete understanding of the anomalous conductivity increase in these oxy-sulfide glasses. Our approach here will be to use simpler oxide additions where we simply substitute oxygen for sulfur without adding any Li cations to the glass so that if the conductivity does increase, then the added complication of an increasing number of alkali cations will be mitigated and the conductivity increase can be more completely and thoroughly understood on the basis of purely structural (mobility) changes to the glass.

Among many possible sulfide glass network formers to choose from for this study, such as SiS_2 , GeS_2 , B_2S_3 , and P_2S_5 , GeS_2 glass has been chosen as the primary glass former for our investigation. This glass former can be used to create ionic

* To whom correspondence should be addressed. Phone: (515) 294-0745. Fax: (515) 294-5444. E-mail: swmartin@iastate.edu.

TABLE 1: Various GeS_2 -Based Lithium Sulfide Glasses Exhibiting High Ionic Conductivity

compositions	$\sigma_{25^\circ\text{C}} (\Omega \text{ cm})^{-1}$	$\Delta E_{\text{act}} (\text{eV})$	glass type ^a	ref
0.5 Li_2S –0.5 GeS_2	4.0×10^{-5}	0.51	R	13
0.63 Li_2S –0.37 GeS_2	1.5×10^{-4}	0.34	TR	14
0.3 Li_2S –0.45 GeS_2 –0.25 SiS_2	1.7×10^{-4}	0.33	TR	15
0.526 Li_2S –0.211 GeS_2 –0.263 Ga_2S_3	1.6×10^{-4}		GF	16
0.58 Li_2S –0.39 GeS_2 –0.03 Li_3PO_4	3.0×10^{-4}		LN	8
0.48 Li_2S –0.48 GeS_2 –0.04 Li_4SiO_4	3.4×10^{-4}		TR	17
0.24 Li_2S –0.36 GeS_2 –0.40 LiI	1.2×10^{-4}	0.47	R	18
0.24 Li_2S –0.36 GeS_2 –0.36 LiI –0.04 LiBr	2.0×10^{-4}	0.48	R	19
0.225 Li_2S –0.225 GeS_2 –0.5 LiI –0.05 Ga_2S_3	1.7×10^{-3}	0.31	R	20

^a R: room-temperature quenching. TR: twin roller quenching. GF: glassy thin film. LN: liquid nitrogen quenching.

glasses with high conductivity and good stability in contact with lithium metal, but it is also not hygroscopic while the other glass formers are extremely unstable in air. For example, when the $\text{Li}_2\text{S} + \text{SiS}_2$ glass is exposed to air, it immediately reacts with air to produce toxic H_2S gas while GeS_2 -based glasses such as $\text{Li}_2\text{S} + \text{GeS}_2 + \text{Ga}_2\text{S}_3$, $\text{Li}_2\text{S} + \text{GeS}_2 + \text{La}_2\text{S}_3$, and $\text{Li}_2\text{S} + \text{GeS}_2 + \text{GeO}_2$ glasses remained stable for several hours without immediately noticeable changes.^{9,12} Hence, this feature will not only improve the ease of handling these glasses in air, but also make them more practical candidates for future commercial utilization in Li batteries.

First, we searched and found various GeS_2 -based lithium glasses exhibiting high conductivity of $\sim 10^{-3}$ to $10^{-4} (\Omega \text{ cm})^{-1}$,^{8,13–20} and these glasses are shown in Table 1. LiI -doped glasses show the highest conductivity as expected, but they have been excluded in our investigations due to the instability of LiI in contact with Li metal.^{5–7} As discussed above, another way to improve the conductivity is by doping lithium oxides into $\text{Li}_2\text{S} + \text{GeS}_2$ binary glasses and the conductivity increases are shown in Table 1. For example, the addition of 3 mol % of Li_3PO_4 (or 4 mol % of Li_4SiO_4) to a $\text{Li}_2\text{S} + \text{GeS}_2$ glass system significantly increases the conductivity and gives the glass good chemical stability in contact with Li metal.^{8,17} Such improvements in the ionic conductivity have been reported to be the result of creating “preferential and structural changes by adding lithium oxide”.^{8,10,11} However, it is not clear whether an increase in the conductivity of Li_3PO_4 - or Li_4SiO_4 -doped glasses is the result of increasing the lithium content or the appearance of favorable structures for the conductivity in the glass matrix.

To eliminate the added complication of the Li oxysalt addition increasing the Li concentration, GeO_2 was added systematically to the FIC 0.5 $\text{Li}_2\text{S} + 0.5\text{GeS}_2$ glass system. We have already reported on the structural changes to the base 0.5 $\text{Li}_2\text{S} + 0.5\text{GeS}_2$ glass caused by the addition of GeO_2 using IR and Raman spectra spectroscopy.²¹ It was found that when GeO_2 replaces GeS_2 in 0.5 $\text{Li}_2\text{S} + 0.5\text{GeS}_2$, which consists of germanium tetrahedra having two bridging and two nonbridging sulfurs, the bridging sulfurs are replaced by oxygen atoms to form bridging oxygens. After replacing all of the bridging sulfurs in the glass, further addition of GeO_2 leads to the formation of nonbridging oxygens.

In this work, the ionic conductivities of 0.5 $\text{Li}_2\text{S} + 0.5[(1 - x)\text{GeS}_2 + x\text{GeO}_2]$ glasses have been investigated. It was found that a 5 mol % addition of GeO_2 improved the ionic conductivity of the 0.5 $\text{Li}_2\text{S} + 0.5\text{GeS}_2$ glass, but further additions of GeO_2 decreased the ionic conductivity. Since the amount of Li^+ ions in the glass was purposefully held constant with this substitution, the observed increase in the conductivity must be caused by purely structural changes in the glass. The relationship between the structural changes caused by the addition of GeO_2 as previously examined by IR and Raman spectroscopy (Ge not being an NMR active nuclei) and ionic conductivities in 0.5 Li_2S

+ 0.5 $[(1 - x)\text{GeS}_2 + x\text{GeO}_2]$ glasses will be correlated in an effort to determine the structural origin of the anomalous conductivity increase in these glasses.

2. Experiments Section

2.1. Sample Preparation. Vitreous GeS_2 was prepared by mixing and reacting stoichiometric amounts of germanium (Cerac, 99.999%) and sulfur (Cerac, 99.999%) in an evacuated silica tube. The silica tube was rotated at ~ 5 rpm at an angle of $\sim 10^\circ$ in a tube furnace and heated at 1 deg/min to 900 $^\circ\text{C}$, held for ~ 8 h, and then quenched in air.

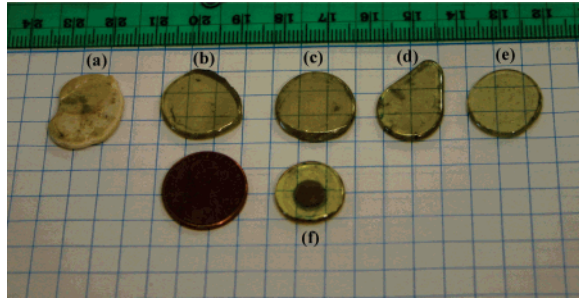
Ternary $\text{Li}_2\text{S} + \text{GeS}_2 + \text{GeO}_2$ glasses were prepared by melting stoichiometric amounts of Li_2S (Cerac, 99.9%), GeS_2 , and GeO_2 (Cerac, 99.999%) starting materials. They were mixed and then placed in a covered vitreous carbon crucible and heated for 5 min between 900 and 1000 $^\circ\text{C}$ inside a hermetically sealed tube furnace attached to the outside of a nitrogen-filled glovebox (<0.1 ppm O_2 and <0.5 ppm H_2O). Although the vapor pressure of both Li_2S and GeS_2 is high, the vapor pressure of the mixture seems to be dramatically decreased when Li_2S and GeS_2 powders are mixed well and melted, especially for high Li_2S content glasses. Weight losses of the samples after melting for 5 min were observed to be less than 2% for all samples. Therefore, the batched glass compositions are not significantly changed during melting and cooling. The molten samples were poured onto a brass mold held 30 to 50 $^\circ\text{C}$ below the glass transition temperature (~ 300 $^\circ\text{C}$, see Table 2), allowed to anneal for 1 h, and then cooled to room temperature at a rate of 1 deg/min. Homogeneous disc-type bulk glasses, ~ 1.5 mm in thickness and ~ 18 mm in diameter, were prepared in this manner. The color changed from transparent yellow to white-yellow with increasing GeO_2 concentration as shown in Figure 1.

2.2. Density Measurements. Density measurements were performed by using the Archimedes method inside the glovebox with kerosene as the suspending liquid.²² The dry mass of the sample was first recorded, and then the mass of the sample was taken submersed in liquid kerosene. Each composition was measured individually three times by using different pieces from the same sample. The density values were found by averaging the three measurements taken for each composition. The errors in the density measurements were estimated by including the largest and smallest values measured.

2.3. Ionic Conductivity Measurements. The thin disk glasses were dry polished to 4000 grit inside the glovebox to improve the electrode/glass contact surface, sputtered with ~ 5 mm diameter gold electrodes (~ 1 μm thick), and placed into an airtight sample chamber for the conductivity measurements. The sample chamber was designed to be able to cover the temperature range of -190 to 500 $^\circ\text{C}$ in helium gas atmosphere for air-sensitive samples.²³ The chamber works by passing helium

TABLE 2: Glass Transition, Density, Molar Volume, Atomic Volume, Free Volume, Ionic Conductivity at Room Temperature, and Activation Energy for $0.5\text{Li}_2\text{S} + 0.5[(1-x)\text{GeS}_2 + x\text{GeO}_2]$

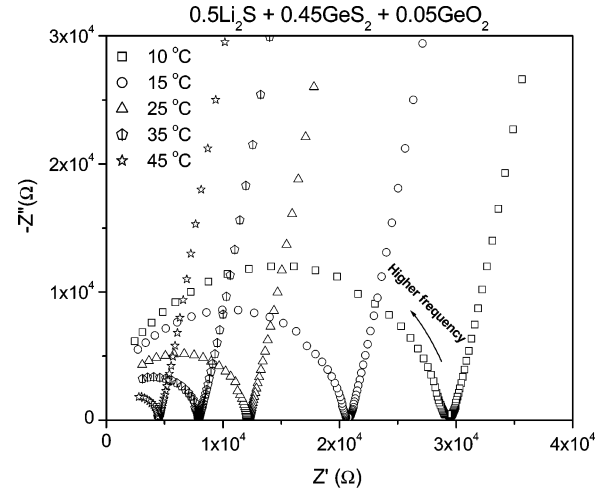
$x\text{GeO}_2$	T_g (°C) (± 5)	ρ (g/cm ³) (± 0.05)	\bar{V}_{mol} (cm ³ /mol) (± 0.75)	\bar{V}_{atom} (cm ³ /mol) (± 0.7)	\bar{V}_{free} (cm ³ /mol) (± 0.7)	$\sigma_{25^\circ\text{C}}$ ($\Omega\text{ cm}$) ⁻¹	ΔE_a (eV) (± 0.006)	$\log \sigma_0$
$x = 0.0$	295	2.45	37.28	24.19	13.09	4.0×10^{-5} [ref 13] 3.3×10^{-5} [ref 14] $\sim 4.26 \times 10^{-5}^a$	0.51 [ref 13] 0.35 [ref 14] $\sim 0.385^a$	4.21 [ref 13] 1.40 [ref 14] $\sim 1.80^a$
$x = 0.1$	297	2.46	36.48	23.27	13.21	$2.23(\pm 0.3) \times 10^{-4}$	0.358	2.38
$x = 0.2$	301	2.48	35.54	22.38	13.16	$8.42(\pm 0.4) \times 10^{-5}$	0.372	2.22
$x = 0.4$	313	2.59	32.79	20.60	12.19	$6.58(\pm 0.8) \times 10^{-5}$	0.391	2.43
$x = 0.6$	321	2.73	29.93	18.89	11.04	$2.56(\pm 0.6) \times 10^{-5}$	0.430	2.67
$x = 0.8$	351	2.82	27.83	17.12	10.71	$4.56(\pm 0.8) \times 10^{-6}$	0.479	2.72

^a Extrapolated value.**Figure 1.** Disc-type glasses ~ 1.5 mm thick and ~ 18 mm in diameter for $0.5\text{Li}_2\text{S} + 0.5[(1-x)\text{GeS}_2 + x\text{GeO}_2]$ for $x = 0.0$ (a), 0.1 (b), 0.2 (c), 0.4 (d), and 0.6 (e) from left. The $0.5\text{Li}_2\text{S} + 0.5\text{GeS}_2$ ($x = 0.0$) glass completely crystallized on normal quenching. The $x = 0.2$ glass (f) was sputtered with gold electrodes ~ 5 mm in diameter for ionic conductivity measurements.

gas through a liquid nitrogen-cooled cooper coil, through a process tube heater, then finally into the sample compartment. The sample chamber was then connected to a previously calibrated Solarton 1260 Impedance Gain-Phase Analyzer to measure the magnitude and phase angle of the impedance of the sample. The complex impedance of the samples was measured from -50 to 200 °C over a frequency range from 0.01 Hz to 10 MHz, using an amplitude voltage of 0.05 V across the sample.

3. Results and Discussion

3.1. Preparation of Bulk Glass Disks for Ionic Conductivity Measurements. For ionic conductivity measurements, homogeneous disc-type glasses (~ 1.5 mm thick and 18 mm diameter) of $0.5\text{Li}_2\text{S} + 0.5[(1-x)\text{GeS}_2 + x\text{GeO}_2]$ compositions have been prepared by quenching the melts on the hot plate mold followed by annealing for 1 h and then cooling them to room temperature at 1 deg/min in a N_2 glovebox. However, the $x = 0$ ($0.5\text{Li}_2\text{S} + 0.5\text{GeS}_2$) glass disk could not be prepared with this method because it completely crystallized on annealing as shown in Figure 1a. In our previous work, thin glass pieces of the $0.5\text{Li}_2\text{S} + 0.5\text{GeS}_2$ could be prepared by rapidly quenching the melts between two cold plates for IR and Raman measurements,²¹ but these glass pieces were too small to be used for ionic conductivity measurements. However, conductivity measurements on disc-shaped glass pieces of $0.5\text{Li}_2\text{S} + 0.5\text{GeS}_2$ with 8 to 10 mm diameter and 1 to 2 mm thickness have been reported in the literature produced by rapid quenching methods.¹³ It was also reported that a twin roller quenching technique,¹⁴ which enables a cooling rate faster than that of rapid air quenching or liquid nitrogen quenching, provided a flake-type glass with ~ 50 μm thickness for conductivity measurements. However, in our experience quenching the melts on a heated brass plate mold in the N_2 glovebox was not fast enough

**Figure 2.** Nyquist plot of the complex impedance for the $0.5\text{Li}_2\text{S} + 0.45\text{GeS}_2 + 0.05\text{GeO}_2$ glass. The frequency increases for each point from right to left starting at 0.1 Hz and finishing at 10 MHz.

to prepare a suitable bulk glass for ionic conductivity measurements.

Therefore to provide accurate data for the $x = 0$ composition conductivity point on samples prepared in exactly the same manner, a series of lower alkali content of $z\text{Li}_2\text{S} + (1-z)\text{GeS}_2$ glasses, with $z = 0.35, 0.4$, and 0.45 , were prepared to provide an accurate value for the $x = 0$ glass by extrapolation. When GeO_2 is added to this glass, good transparent bulk glasses could be prepared as shown in Figure 1. The color changed from transparent yellow to white-yellow with increasing GeO_2 concentration.

3.2. Ionic Conductivities of $0.5\text{Li}_2\text{S} + 0.5[(1-x)\text{GeS}_2 + x\text{GeO}_2]$ Glasses. Figure 2 shows typical complex impedance plots for the $x = 0.1$ ($0.5\text{Li}_2\text{S} + 0.45\text{GeS}_2 + 0.05\text{GeO}_2$) glass. The semicircle at high frequency represents the bulk response of the glass to an applied electric field. The bulk resistance was obtained from the intersection of the semicircle with the real (Z') axis at the lower frequency side. The obtained resistances were converted to the dc conductivities by using the cell constant (sample thickness/electrode area) of the prepared glasses. The beginning of a second arc seen at lower frequencies is believed to be due to space charge polarization effects at the electrodes.

The temperature dependence of the ionic conductivities for the $0.5\text{Li}_2\text{S} + 0.5[(1-x)\text{GeS}_2 + x\text{GeO}_2]$ glasses are presented in Figure 3. For all glass samples, the conductivity increases following an Arrhenius behavior, $\sigma(T) = \sigma_0 \exp(-\Delta E_a/RT)$, over the measured temperature range. The activation energy of conduction, ΔE_a , was calculated from the slope obtained from the $\log(\sigma)$ versus $1/T$ plot. These values are listed along with the conductivities at room temperature in Table 2. In the case of the $0.5\text{Li}_2\text{S} + 0.5\text{GeS}_2$ glass, a suitable bulk glass for

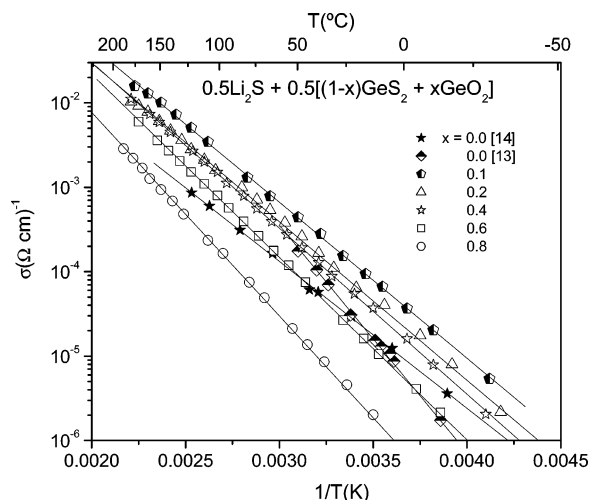


Figure 3. Variation of the ionic conductivity with temperature for $0.5\text{Li}_2\text{S} + 0.5[(1-x)\text{GeS}_2 + x\text{GeO}_2]$ glasses and compared with that of $0.5\text{Li}_2\text{S} + 0.5\text{GeS}_2$ glass prepared by twin roller quenching¹⁴ and rapid quenching methods.¹³ The slopes of the Arrhenius plots for $0.5\text{Li}_2\text{S} + 0.5\text{GeS}_2$ glass are very different depending on the quenching rate, which gives different activation energies.

conductivity measurements could not be prepared by our quenching method as described above. However, the conductivity and activation energy of this composition glass have been reported in the literature.^{13,14} The conductivities ($\sigma_{25^\circ\text{C}}$) of the $0.5\text{Li}_2\text{S} + 0.5\text{GeS}_2$ glass prepared by rapid quenching and twin roller quenching methods were reported to be 4.0×10^{-5} and $3.5 \times 10^{-5} (\Omega \text{ cm})^{-1}$, respectively. Since these values were quite similar, the conductivity of this glass may not strongly depend on the cooling rate. However, the activation energy of $0.5\text{Li}_2\text{S} + 0.5\text{GeS}_2$ glass was significantly affected by the quenching rate:¹⁴ 0.51 eV for the glass prepared in the rapid quenching method and 0.35 eV for the glass prepared in the twin roller quenching method. A similar behavior was also observed in silicate glasses where an increase in cooling rate was found to decrease the activation energy.²⁴

Hence, to more accurately determine the activation energy and conductivity of the binary $0.5\text{Li}_2\text{S} + 0.5\text{GeS}_2$ glass so that it can be compared with the value of our oxy-sulfide glasses prepared with our quenching method, $z\text{Li}_2\text{S} + (1-z)\text{GeS}_2$ ($z = 0.35, 0.4$, and 0.45) glasses have been prepared by using the identical quenching and annealing processes that were used to prepare the oxy-sulfide glasses. All the glasses in this study were carefully prepared by using the same quenching rate, annealing temperature and time, and cooling rate to room temperature to minimize the effect of quenching rate on activation energy. Figure 4 shows the conductivities and activation energies of the $z\text{Li}_2\text{S} + (1-z)\text{GeS}_2$ ($z = 0.35, 0.4$, and 0.45) glasses and these values are listed in Table 3. From these data, an ionic conductivity of $\sim 4.3 \times 10^{-5} (\Omega \text{ cm})^{-1}$ and the activation of ~ 0.385 eV are extrapolated for the $0.5\text{Li}_2\text{S} + 0.5\text{GeS}_2$ glass as shown in Figure 4. This conductivity is very comparable with 4.0×10^{-5} and $3.5 \times 10^{-5} (\Omega \text{ cm})^{-1}$ previously reported in the literature. However, the activation energy of ~ 0.385 eV is different from those (0.35 and 0.54 eV) reported in the literature and is most likely caused by the different quenching rate used in the different studies.

The ionic conductivity at 25°C ($\sim 4.3 \times 10^{-5} (\Omega \text{ cm})^{-1}$) of the $0.5\text{Li}_2\text{S} + 0.5\text{GeS}_2$ ($x = 0$) glass is improved to $1.5 \times 10^{-4} (\Omega \text{ cm})^{-1}$ by addition of 5 mol % of GeO_2 . However, further additions of GeO_2 monotonically decrease the conductivity ($\sigma_{25^\circ\text{C}}$) as shown in Figure 5. At the same time, the activation

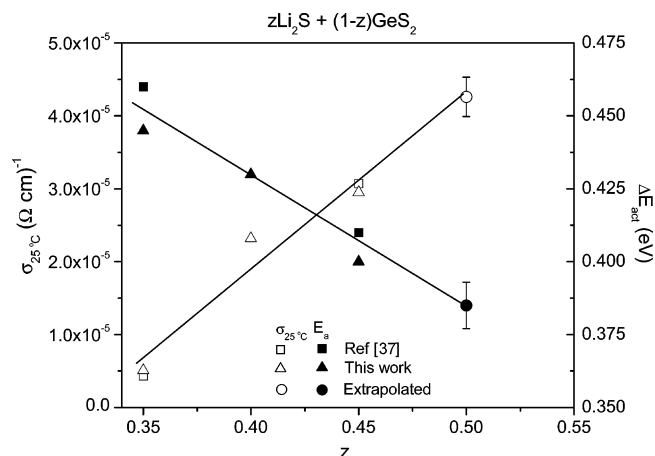


Figure 4. Extrapolated ionic conductivities and activation energies for the $0.5\text{Li}_2\text{S} + 0.5\text{GeS}_2$ glass from those of $z\text{Li}_2\text{S} + (1-z)\text{GeS}_2$ glasses ($z = 0.35, 0.4, 0.45$).

TABLE 3: Ionic Conductivities at Room Temperature and Activation Energies for $z\text{Li}_2\text{S} + (1-z)\text{GeS}_2$ Glasses^a

compositions	$\sigma_{25^\circ\text{C}} (\Omega \text{ cm})^{-1}$	ΔE_a (eV) (± 0.006)	$\log \sigma_0$ (± 0.08)
$0.35\text{Li}_2\text{S} + 0.75\text{GeS}_2$	5.08×10^{-6} (4.33×10^{-6}) ³⁷	0.44 (0.46) ³⁷	2.14
$0.4\text{Li}_2\text{S} + 0.6\text{GeS}_2$	2.32×10^{-5}	0.43	2.02
$0.45\text{Li}_2\text{S} + 0.65\text{GeS}_2$	2.95×10^{-5} (3.07×10^{-5}) ³⁷	0.40 (0.41) ³⁷	1.92
$0.5\text{Li}_2\text{S} + 0.5\text{GeS}_2$	$\sim 4.26 \times 10^{-5}$ ^b	~ 0.385 ^b	~ 1.80 ^b

^a $z = 0.35, 0.4$, and 0.45 glasses were prepared at identical conditions the oxy-sulfide glasses have taken to extrapolate the conductivity and activation of $x = 0.5$ glass. ^b Extrapolated value.

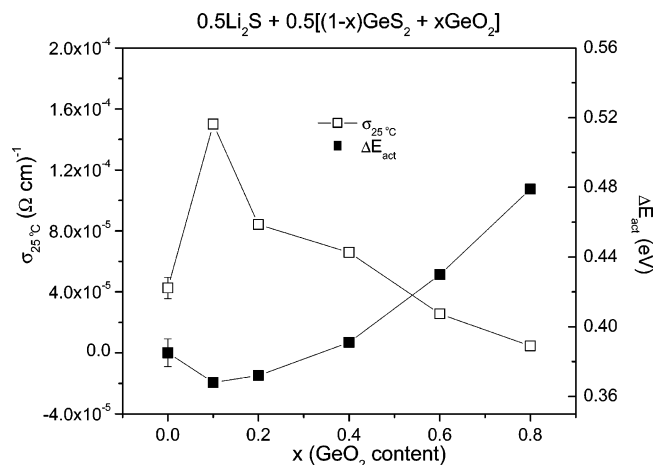


Figure 5. The ionic conductivities ($\sigma_{25^\circ\text{C}}$) and activation energies (ΔE_a) for the $0.5\text{Li}_2\text{S} + 0.5[(1-x)\text{GeS}_2 + x\text{GeO}_2]$ glasses ($0.1 \leq x \leq 0.8$). Data for the $x = 0$ glass was obtained by extrapolation in Figure 4.

energy first decreases when 5 mol % of GeO_2 is added, but it then increases with increasing GeO_2 contents (Figure 5). However, in $(1-x)(0.6\text{Li}_2\text{S} + 0.4\text{SiS}_2) + x\text{Li}_4\text{SiO}_4$ glasses, the addition of 5 mol % of Li_4SiO_4 to the $0.6\text{Li}_2\text{S} + 0.4\text{SiS}_2$ glass increased the ionic conductivity and also increased the activation energy.^{10,25,26} Tatsumisago et al.¹⁰ suggested that such enhancement of lithium ion conductivity was caused by the appearance of a unique glass structure. On the other hand, Kawakami et al.²⁵ reported that the increased ionic conductivity was due to increasing the concentration of mobile Li^+ ions by doping 5 mol % of Li_4SiO_4 . In our case, since the amount of Li^+ ions is constant and the activation energy initially decreases with added oxygen, the observed improvement in the conductivity

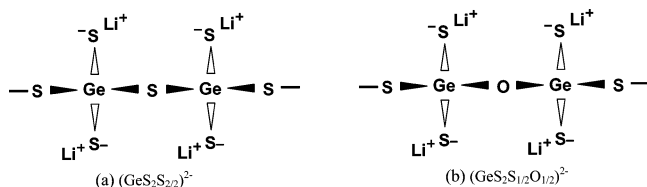


Figure 6. The structural units for (a) $0.5\text{Li}_2\text{S} + 0.5\text{GeS}_2$ glass and (b) $0.5\text{Li}_2\text{S} + 0.45\text{GeS}_2 + 0.05\text{GeO}_2$ glass. Added GeO_2 to $0.5\text{Li}_2\text{S} + 0.5\text{GeS}_2$ glass causes the formation of $\text{Ge}-\text{O}-\text{Ge}$ bridging units.

ity must be caused by a structural change to the glass that in turn leads to a decrease in the activation energy.

3.3. Structure Effects on the Activation Energy of $0.5\text{Li}_2\text{S} + 0.5[(1-x)\text{GeS}_2 + x\text{GeO}_2]$ Glasses. In our previous work, the structures of $0.5\text{Li}_2\text{S} + 0.5[(1-x)\text{GeS}_2 + x\text{GeO}_2]$ glasses were investigated with Raman and IR spectroscopy.²¹ The binary $0.5\text{Li}_2\text{S} + 0.5\text{GeS}_2$ glass consists of germanium tetrahedral units with two bridging and two nonbridging sulfurs (Figure 6a). When GeO_2 is added to the $0.5\text{Li}_2\text{S} + 0.5\text{GeS}_2$ glass, it was found that the added oxygen atoms replace the bridging sulfur atoms first instead of the nonbridging sulfur atoms. In other words, the oxygen ions favor the higher field strength Ge^{4+} cation over the lower field strength Li^+ cation to form bridging oxygens with the Ge^{4+} cations rather than to form nonbridging oxygens with the Li^+ cations. Figure 6b shows the structural unit of $0.5\text{Li}_2\text{S} + 0.45\text{GeS}_2 + 0.05\text{GeO}_2$ glass, which consists of germanium tetrahedra with one bridging oxygen, one bridging sulfur, and two nonbridging sulfurs. Because the Li^+ ions are still associated with the sulfur units, which helps to maintain their high mobility in the 5 mol % GeO_2 doped glass, the ionic conductivity is not diminished. On the other hand, had the small amounts of oxygen atoms introduced to the glass structure created nonbridging oxygen atoms, the conductivity would be expected to decrease since nonbridging oxygens are known to be strong lithium ion traps²⁷ and a higher conductivity would not be expected in the $0.5\text{Li}_2\text{S} + 0.45\text{GeS}_2 + 0.05\text{GeO}_2$ glass. Therefore, the creation of the bridging oxygens by the addition of GeO_2 with the nonbridging sulfurs may be the major cause of the increase of conductivity.

To obtain a deeper understanding of the increase in the conductivity of the $0.5\text{Li}_2\text{S} + 0.45\text{GeS}_2 + 0.05\text{GeO}_2$ glass as a result of structural changes to the glass, the Anderson and Stuart model²⁸ has been considered. In alkali ion conducting alkali silicate glasses, Anderson and Stuart suggested that the total activation energy, ΔE_{act} , is the result of two contributions:

$$\Delta E_{\text{act}} = \Delta E_{\text{B}} + \Delta E_{\text{S}} \quad (1)$$

where ΔE_{B} is the electrostatic binding energy and ΔE_{S} is the strain energy. The electrostatic contribution, ΔE_{B} , is the energy required to separate the mobile cation ion from its charge-compensating anion site and was given the form

$$\Delta E_{\text{B}} = \frac{1}{\gamma} \left(\frac{ZZ_{\text{O}}e^2}{r + r_{\text{O}}} - \frac{ZZ_{\text{O}}e^2}{\lambda/2} \right) \quad (2)$$

where γ is a covalence parameter related to the deformability of the oxygen ion (in oxide glasses); Z_{e} and Z_{Oe} are the electrical charges of the lithium and oxide ions, respectively; r and r_{O} are the ionic radii of cation and oxide (in an oxide glass) ions, respectively; and λ is the jump distance. In the case of $0.5\text{Li}_2\text{S} + 0.45\text{GeS}_2 + 0.05\text{GeO}_2$ glass, ΔE_{B} is the energy required to separate the Li^+ ion from the nonbridging sulfur to which it was bonded and move it halfway to an adjacent nonbridging

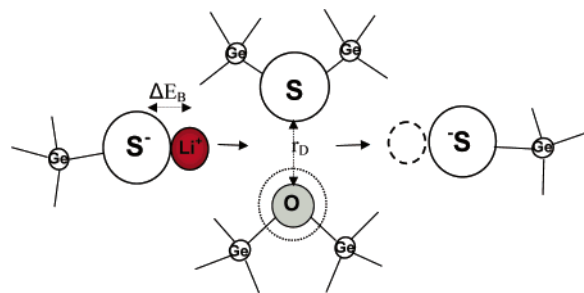


Figure 7. Simplified pictorial view of the ionic conduction energy for $0.5\text{Li}_2\text{S} + 0.45\text{GeS}_2 + 0.05\text{GeO}_2$ glass (after Martin et al.²⁹). Ionic conduction requires the electrostatic binding energy (ΔE_{B}) to separate the Li^+ ion from its charge compensating anion site and move to the next site and the strain energy (ΔE_{S}) to open up doorways (r_{D}) in the structure large enough for the ions to pass through.

sulfur and the various distance parameters would be changed to values approximate for a sulfide glass.

Martin and Angell²⁹ have presented an energy landscape interpretation of the Anderson and Stuart energy barrier model and this is shown in Figure 7. The γ parameter is used to determine the covalent nature of $\text{O}(\text{S})-\text{Li}$ bonds. In the special case of these particular glasses, the modifier Li contents are not changed with the addition of GeO_2 to the $0.5\text{Li}_2\text{S} + 0.5\text{GeS}_2$ glass and hence the covalent nature of the $\text{S}-\text{Li}$ bonds would be constant, which would yield a constant γ value. The jump distance, λ , which normally decreases with increasing modifier content, is related to the distance between two nonbridging sulfurs ions in the glasses. Again, in the case here where the total modifier content is unchanged, the jump distance (λ) is also considered to be constant (or at most change slowly and monotonically). Since we have given reasonable evidence to suggest that the terms in the binding energy are unchanged (or change little) with added GeO_2 , the binding energy term can be considered to be constant when 5 mol % of GeO_2 is added to $0.5\text{Li}_2\text{S} + 0.5\text{GeS}_2$ glass. Therefore, this leads us to consider the strain energy term to be the only probable cause of the decrease in total activation energy, which in turn leads to the increase in the conductivity.

The strain energy, ΔE_{S} , is the energy required to strain the “doorways” in the structure large enough for the mobile ions to pass through them. Anderson and Stuart have approximated the strain energy using Frenkel’s equation,³⁰ but this has been revised by McElfresh et al.³¹ to give a better approximation to strain energy during the conduction event:³²

$$\Delta E_{\text{S}} = \pi G(r - r_{\text{D}})^2(\lambda/2) \quad (3)$$

where r is the cation radius, r_{D} is the “doorway” radius in the glass, G is the shear modulus of the glass, and λ is the jump distance of the diffusing species. The two terms in the strain energy that would be considered to change the most with the addition of GeO_2 to the $0.5\text{Li}_2\text{S} + \text{GeS}_2$ glass would be G and r_{D} . The jump distance would change very little since the concentration of Li^+ ion remains the same. While neither of these former values is known exactly for these glasses, we can make reasonable arguments for how they would change with added GeO_2 . Since the shear modulus G normally follows the glass transition temperature,^{32,33} the trends of the shear modulus can be expected from changes of the glass transition temperatures with increasing GeO_2 concentration in $0.5\text{Li}_2\text{S} + 0.5\text{GeS}_2$ glass. As seen in Table 2, the glass transition temperatures increase only slightly with increasing GeO_2 content in $0.5\text{Li}_2\text{S} + 0.5[(1-x)\text{GeS}_2 + x\text{GeO}_2]$ glasses so it is expected that the

TABLE 4: The Calculated Doorway Radii of $0.5\text{Li}_2\text{S} + 0.5[(1-x)\text{GeS}_2 + x\text{GeO}_2]$ Glasses^a

	$x\text{GeO}_2 =$			
	0.0	0.1	0.2	0.4
ΔE_A (eV)	0.385	0.358	0.372	0.391
ΔE_B (eV)	0.315	0.315	0.315	0.315
ΔE_S (eV)	0.07	0.043	0.057	0.076
r_D (Å)	0.30	0.37	0.33	0.29

^a The strain energy of $x = 0.0$ glass is assumed to be 0.07 eV, the expected shear modulus of the glasses, G , is 2×10^{10} (N/m²), the jump distance of Li^+ in the glasses, λ , is ≈ 3.96 Å, and the ionic radius of Li, $r(\text{Li}^+)$, is 0.6 Å.

shear modulus would increase slightly as well. Hence, a decreasing G value with added GeO_2 is not likely the cause for a decrease in the strain energy.

Therefore, the “doorway” radius (r_D) is considered to be a likely factor for decreasing the strain energy, resulting in the decrease in the total activation energy. The doorway radius can be calculated by using eq 3 if the jump distance (λ), the shear modulus (G), and the strain energy are obtained. The jump distance (λ) is estimated to be 3.96 Å from the alkali ion concentration and the molar volume of the glasses. For example, for the $0.5\text{Li}_2\text{S} + 0.5\text{GeS}_2$ glass, N_{Li^+} (number of Li ions per unit volume) = moles of Li^+ /molar volume of the glass = 1.625×10^{22} Li^+/cm^3 . Then, V_{Li^+} (the volume occupied by one Li^+ ion) = $1/(1.625 \times 10^{22} \text{ Li}^+/\text{cm}^3) = 0.619 \times 10^{-22} \text{ cm}^3/\text{Li}^+$. When it is assumed that each lithium atom occupies the center of a cubic lattice, the distance between Li^+ ions (d_{Li^+}) = $(V_{\text{Li}^+})^{1/3} = (0.619 \times 10^{-22} \text{ cm}^3)^{1/3} = 3.96$ Å. Unfortunately, the shear modulus (G) has not been measured for this glass system, but an estimate can be obtained from the shear modulus (2×10^{10} (N/m)) of the $\text{Ag}_2\text{S} + \text{GeS}_2$ system³⁴ because the glass transitions of the $\text{Li}_2\text{S} + \text{GeS}_2$ system are similar to those of the $\text{Ag}_2\text{S} + \text{GeS}_2$ system.³⁵ We assumed in the above discussion that the binding energy term of the $x = 0$ glass does not change significantly with small additions of GeO_2 content because the covalent nature (γ) of the S - Li bonds and the jump distance (λ) of the Li^+ ions are thought to be approximately constant. However, for the $x > 0.5$ glasses, γ would be changed since the nonbridging oxygen appears.²¹ Therefore, if we know (or can estimate) the binding energy for the $x = 0$ glass, the strain energies of $x = 0.1, 0.2$, and 0.4 glasses can be obtained by subtracting the binding energy for the $x = 0$ glass from their total activation energies. Alternatively, when the strain energy of the $x = 0$ glass is assumed to be ~ 0.07 eV (it has been estimated to be 0.07 eV for $\text{Ag}_2\text{S} + \text{GeS}_2$ glass),³⁴ the strain energies for the $x = 0.1, 0.2$, and 0.4 glasses can be calculated to be 0.043, 0.057, and 0.076 eV, respectively and these results are shown in Table 4. By using the above jump distance (calculated from cation concentration and molar volume), shear modulus, and the strain energies, the doorway radii for the $x = 0.0, 0.1, 0.2$, and 0.4 glasses were calculated by using eq 3. For example, the doorway radius of $0.5\text{Li}_2\text{S} + 0.5\text{GeS}_2$ glass ($x = 0.0$) is 0.30 Å. This increases to 0.37 Å by adding 0.05GeO_2 . Further additions of GeO_2 decrease the doorway radius: 0.33 Å for 0.1GeO_2 and 0.29 Å for 0.2GeO_2 . Different strain energy values between 0.04 and 0.20 eV were then used to determine the trends of doorway radius with increasing GeO_2 as shown in Figure 8. For all of the different strain energies, the doorway radius increases with the addition of 0.05GeO_2 and then decrease gradually by further additions of GeO_2 .

We have shown that GeO_2 additions cause the formation of bridging oxygens in the $0.5\text{Li}_2\text{S} + 0.45\text{GeS}_2 + 0.05\text{GeO}_2$ glass (Figure 6). Since the replaced oxygen atoms are smaller than

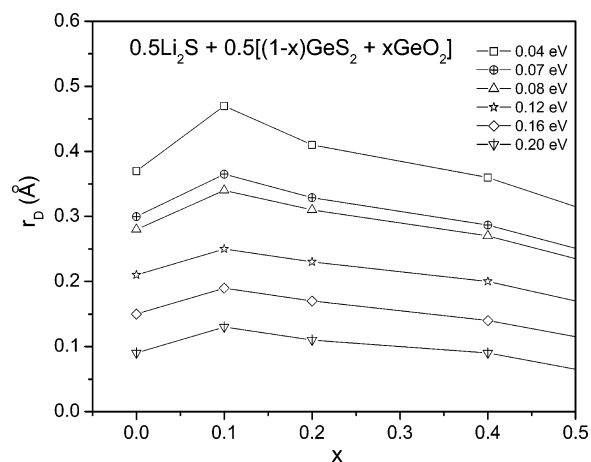


Figure 8. The calculated doorway radii of $0.5\text{Li}_2\text{S} + 0.5[(1-x)\text{GeS}_2 + x\text{GeO}_2]$ glasses when the strain energy of $x = 0.0$ glass is assumed to range from 0.04 to 0.2 eV.

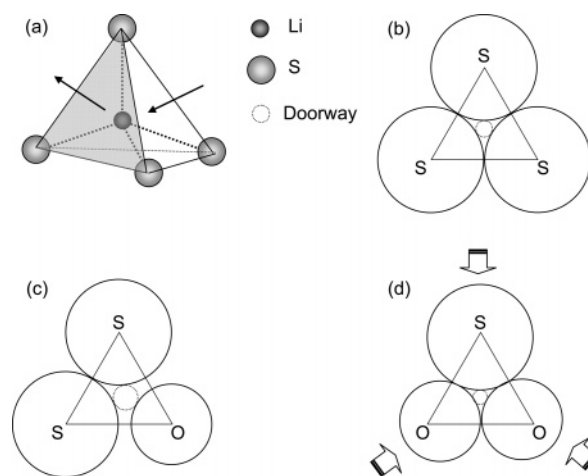


Figure 9. (a) Schematic diagram of the tetrahedral (consisting of sulfide anions) site where the Li^+ ion is located: The Li^+ ionic conduction path is from the centroid of the tetrahedral site, through one of the triangular faces comprising the doorway and to the centroid of the neighboring tetrahedral site. (b) Schematic diagram of the doorway site at the center of the triangular faces consisting of three sulfur anions. The doorway radius is calculated to be 0.29 Å. (c) The doorway site is comprised of two sulfur anions and one oxygen anion. $r_D = 0.4$ Å. (d) The proposed doorway site for $x \geq 0.4$ glasses. It is comprised of one sulfur and two oxygen anions with a more collapsed structure, which produces a smaller doorway radius, $r_D = 0.24$ Å.

the sulfur atoms, we believe that this may lead to an increased “doorway” radius (r_D). A pictorial representation of this effect is shown in Figure 9. To observe this effect from the point of view of the local structure of the glasses, the structure of the $0.5\text{Li}_2\text{S} + 0.5\text{GeS}_2$ glass is first regarded as a quasidense packing of the sulfur (network-forming) anions based on the analogy to Elliott’s assumption.³⁴ In this structure, the germanium (network-forming) cations occupy some of the interstices in the network and the conducting Li^+ ions occupy other interstices. On the basis of the crystal structure of Li_4GeS_4 ,³⁶ the Li^+ ions are assumed to occupy the regular tetrahedral sites in the network structure of the $0.5\text{Li}_2\text{S} + 0.5\text{GeS}_2$ glass. Then, the Li^+ ionic conduction path can be envisioned within ion jumps from one tetrahedral interstice, through one of the triangular faces of the tetrahedron, to the neighboring tetrahedral interstice as shown in Figure 9a. Three sulfur anions on the triangular face comprise the doorways and the schematic diagram of the doorway site at the center of the triangular face is shown in Figure 9b. The doorway radius can be estimated

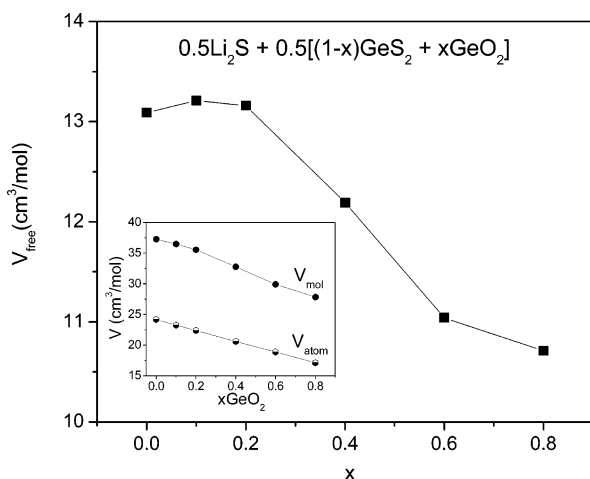


Figure 10. The calculated free volumes (\bar{V}_{free}) of $0.5\text{Li}_2\text{S} + 0.5[(1-x)\text{GeS}_2 + x\text{GeO}_2]$ glasses obtained by subtracting the calculated atomic volumes (\bar{V}_{atomic}) of the constituent elements from the molar volumes (\bar{V}_{molar}).

from the geometry of a tetrahedron. The doorway radius for the $0.5\text{Li}_2\text{S} + 0.5\text{GeS}_2$ glass is calculated to be 0.29 \AA when a Li–S bond distance of 2.3 \AA and S^{2-} ionic radius of 1.84 \AA are used. Li–S bond distances range from ~ 2.3 to $\sim 2.6 \text{ \AA}$ in the crystal structure of Li_4GeS_4 ³⁶ and 2.3 \AA is used in this work. Surprisingly, 0.29 \AA is very similar to the doorway radius (0.30 \AA) obtained by using eq 3 with the strain energy of 0.07 eV .

In the case of the $x = 0.1$ glass, since 6.7% of the sulfur atoms are replaced by the oxygen atoms, some of the tetrahedra in the structure will consist of one oxygen anion and three sulfur anions. When the Li^+ ion moves through the triangular face containing one oxygen anion with two sulfur anions (Figure 9c), the doorway radius is calculated to be 0.40 \AA when the same Li–S bond distance of 2.3 \AA , S^{2-} ionic radius of 1.84 \AA , and O^{2-} radius of 1.4 \AA are used. This value is very comparable to the doorway radius (0.37 \AA) for the $0.5\text{Li}_2\text{S} + 0.45\text{GeS}_2 + 0.05\text{GeO}_2$ glass, which was calculated by using eq 3 with the strain energy of 0.07 eV . For the $x = 0.2$ glass containing 13.3% of the oxygen atoms, although most of the doorway sites are still comprised of two sulfur anions and one oxygen anion (Figure 9c), the number of doorway sites consisting of two oxygen anions and one sulfur anion would increase. In this case, the calculated doorway radius slightly decreases from 0.37 to 0.33 \AA . This value is still larger than that of $x = 0$ glass.

These changes in the doorway radii are very consistent with the changes in the free volume (\bar{V}_{free}) calculated for the glasses. \bar{V}_{free} is calculated by subtracting the calculated atomic volume of the constituent elements in the glass from the molar volume of the glass. Values of \bar{V}_{molar} , \bar{V}_{atomic} , and \bar{V}_{free} are given in Table 2 and they are also shown in Figure 10. From Table 2, it is seen that for the $x = 0$ glass, \bar{V}_{free} is $13.09 \text{ cm}^3/\text{mol}$ and it increases slightly to $13.21 \text{ cm}^3/\text{mol}$ for the $x = 0.1$ glass, but it then decreases slightly to $13.16 \text{ cm}^3/\text{mol}$ for the $x = 0.2$ glass. These values suggest that the network structure is opened slightly by the addition of 0.05GeO_2 , but is collapsed by further additions of GeO_2 . Therefore, for the $x \geq 0.4$ glasses, the \bar{V}_{free} is observed to sharply decrease as shown in Figure 10, which is consistent with the sharp increase in the glass transition temperature regarded as a measure of the shear modulus. The doorway site for higher GeO_2 content glasses ($x \geq 0.4$) is therefore proposed to be collapsed. The doorway site is predominately comprised of one sulfur and two oxygen anions because the glasses contain more than 26.7% of oxygen atoms where the tetrahedron would be expected to consist of two

oxygen and two sulfur anions as shown in Figure 9d. The collapsed doorway radius is calculated to be 0.24 \AA , which is comparable to 0.29 \AA for the $x = 0.4$ glass that was calculated using eq 3. The decrease in the calculated doorway radius, the sharp decrease in the free volume, and the increase in the glass transition temperature strongly suggest that the network structure collapses by substituting additional oxygens beyond $x = 0.05$ for sulfur atoms.

It is also significant to note that for $x > 0.5$ glasses, the binding energy (ΔE_{B}) term is likely not expected to be constant (as it has been assumed for the $x < 0.5$ glasses) because the nonbridging oxygens, strong Li^+ ion traps, would begin to appear for these more highly modified glasses. In addition, the strain energy would be expected to increase due to further decreases in the doorway radius and increases in the shear modulus. These trends may lead to the sharp increase in the total activation energy and hence the sharp decrease in the Li^+ conductivity.

4. Conclusions

The $0.5\text{Li}_2\text{S} + 0.5[(1-x)\text{GeS}_2 + x\text{GeO}_2]$ glasses have been prepared and the effect of added GeO_2 on the conductivity has been studied. For the $0.5\text{Li}_2\text{S} + 0.5\text{GeS}_2$ ($x = 0$) glass, because a bulk glass disk could not be prepared, the ionic conductivity at room temperature and activation energy were extrapolated from those of $z\text{Li}_2\text{S} + (1-z)\text{GeS}_2$ ($0.35 \leq z \leq 0.45$) glasses. The addition of 5 mol % of GeO_2 to the $0.5\text{Li}_2\text{S} + 0.5\text{GeS}_2$ glass increases the ionic conductivity while decreasing the activation energy. Further addition of GeO_2 monotonically increases the activation energy and decreases the conductivity. Unlike other oxy-sulfide glasses such as $\text{Li}_2\text{S} + \text{SiS}_2 + \text{Li}_x\text{MO}_y$, where $\text{Li}_x\text{MO}_y = \text{Li}_3\text{PO}_4$, Li_4SiO_4 , Li_3BO_3 , and Li_4GeO_4 , the amount of Li^+ ions is constant in our glass system so that the effect of variable Li^+ ions on conductivity is excluded from the investigation and hence also as a cause of enhanced conductivity in the $0.5\text{Li}_2\text{S} + 0.45\text{GeS}_2 + 0.05\text{GeO}_2$ glass. The Anderson and Stuart model has been used to explain a decrease in the activation energy when 5 mol % of GeO_2 is added to the $0.5\text{Li}_2\text{S} + 0.5\text{GeS}_2$ glass. A slightly increasing “doorway” radius in the strain energy term is proposed as cause of the decreasing activation energy, which results in increasing ionic conductivity. The calculated doorway radius from an analysis of the local structure of these glasses strongly supports the above hypotheses.

Acknowledgment. This research was supported by the NASA Jet Propulsion Laboratory under grant No. 1250174 and this research support is gratefully acknowledged.

References and Notes

- (1) Mercier, R.; Malugani, J. P.; Fahys, B.; Saida, A. *Solid State Ionics* **1981**, *5*, 663.
- (2) Wada, H.; Menetrier, M.; Levasseur, A.; Hagenmuller, P. *Mater. Res. Bull.* **1981**, *18*, 189.
- (3) Kennedy, J.; Yang, Y. J. *Solid State Chem.* **1987**, *69*, 252.
- (4) Akridge, J. R.; Vourlis, H. *Solid State Ionics* **1986**, *18/19*, 1082.
- (5) Kondo, S.; Takada, K.; Yamamura, Y. *Solid State Ionics* **1992**, *53–56*, 1183.
- (6) Takada, K.; Aotani, N.; Kondo, S. *J. Power Sources* **1993**, *43–44*, 135.
- (7) Kennedy, J. H.; Zhang, Z. *Solid State Ionics* **1988**, *28–30*, 726.
- (8) Yamamura, Y.; Hasegawa, M.; Takada, K.; Kondo, S. European Patent Application, EP 469574, 1992.
- (9) Saienga, J. Ph.D. Thesis, Iowa State University, 2005.
- (10) Tatsumisago, M.; Hirai, K.; Hirata, T.; Takahashi, M.; Minami, T. *Solid State Ionics* **1996**, *86–88*, 487.
- (11) Hayashi, A.; Yamashita, H.; Tatsumisago, M.; Minami, T. *Solid State Ionics* **2002**, *148*, 381.
- (12) Kim, Y. Ph.D. Thesis, Iowa State University, to be published in 2006.

- (13) Ribes, M.; Barrau, B.; Souquet, J. L. *J. Non-Cryst. Solids* **1980**, 38/39, 271.
- (14) Pradel, A.; Pagnier, T.; Ribes, M. *Solid State Ionics* **1985**, 17, 147.
- (15) Deshpande, V. K.; Pradel, A.; Ribes, M. *Mater. Res. Bull.* **1988**, 23, 379.
- (16) Yamashita, M.; Yamanaka, H. *Solid State Ionics* **2003**, 158, 151.
- (17) Minami, T.; Takada, K.; Kondo, S. European Patent Application, EP 618632, 1994.
- (18) Carette, B.; Robinel, E.; Ribes, M. *Glass Technol.* **1983**, 24, 157.
- (19) Carette, B.; Ribes, M.; Souquet, J. L. *Solid State Ionics* **1983**, 9 and 10, 735.
- (20) Saienga, J.; Kim, Y.; Campbell, B.; Martin, S. W. *Solid State Ionics* **2005**, 176, 1229.
- (21) Kim, Y.; Saienga, J.; Martin, S. W. *J. Non-Cryst. Solids* **2005**, 351, 3716.
- (22) Varshneya, A. *Fundamentals of Inorganic Glasses*; Academic Press Inc.: New York, 1994; pp 150.
- (23) Schrooten, J. Ph.D. Thesis, Iowa State University, 2001.
- (24) Tomozawa, M.; Yoshiyagawa, W. *J. Phys. (Paris)* **1982**, 12 [C9], 411.
- (25) Kawakami, Y.; Ikuta, H.; Uchida, T.; Wakihara, M. *Thermochim. Acta* **1997**, 299, 7.
- (26) Hirai, K.; Tatsumisago, M.; Minami, T. *Solid State Ionics* **1995**, 78, 269.
- (27) Hayashi, A.; Hirai, K.; Tatsumisago, M.; Takahashi, M.; Minami, T. *Solid State Ionics* **1996**, 86–88, 539.
- (28) Anderson, O.; Stuart, D. J. *Am. Ceram. Soc.* **1954**, 37, 573.
- (29) Martin, S. W.; Angell, C. A. *Solid State Ionics* **1986**, 23, 185.
- (30) Frenkel, J. *Kinetic Theory of Liquid*; Oxford University Press: New York, 1946; pp 7–11.
- (31) McElfresh, D. K.; Howitt, D. G. *J. Am. Ceram. Soc.* **1986**, 69 [10], C-237.
- (32) Martin, S. W. *J. Am. Ceram. Soc.* **1988**, 71 (6), 438.
- (33) Srinivasarao, G.; Veeraiah, N. *J. Solid State Chem.* **2002**, 166, 104.
- (34) Elliott, S. R. *J. Non-Cryst. Solids* **1993**, 160, 29.
- (35) Souquet, J. L.; Robinel, E.; Barrau, B.; Ribes, M. *Solid State Ionics* **1981**, 3/4, 317.
- (36) Matsushita, Y.; Kanatzidis, M. G. *Z. Naturforsch.* **1998**, B53 (1), 23.
- (37) Kim, K. H.; Torgeson, D. R.; Borsa, F.; Cho, J.; Martin, S. W.; Svare, I. *Solid State Ionics* **1996**, 91, 7.